Title	Performance of Wide-Angle Two-Dimensional Diffusers with Vane Systems (3rd Report)
Author(s)	Yamazato, Eisho; Irabu, Kunio
Citation	琉球大学理工学部紀要. 工学篇 = Bulletin of Science & Engineering Division, University of the Ryukyus. Engineering(8): 1-15
Issue Date	1975-01-30
URL	http://hdl.handle.net/20.500.12000/26215
Rights	

Performance of Wide-Angle Two-Dimensional Diffusers with Vane Systems (3rd Report)

Eisho YAMAZATO*, Kunio IRABU*

In the previous works, experiments were made with flat vanes in diffusers with divergence angles of 30°, 40°, and 60°, and showed the basic criteria for effective vane configurations with source-point translation. In the present work, tests were made with flat vanes in two-dimensional diffusers, to determine the relation between pressure recovery and flow regime.

For the optimum vane configurations with source-point translation on the pressure recovery, the flow regime in the downstream duct is also greatly improved. The area of separation is considerably reduced, and the velocity profiles in the downstream duct can be flattened. However, the section where the velocity profile is to be uniform can be attained at the far distance in the downstream duct, compared with the pressure recovery section.

1. Introduction

In internal flows of fluid in ducts or fluid machineries, it frequently becomes necessary to decrease the fluid velocity and to increase the static pressure. In general, a diffuser flow with small divergence angle results in a smooth flow with high pressure recovery efficiency, low energy loss, and uniform exit velocity profiles. On the other hand, in a short diffuser with large divergence angle, severe flow asymmetry and unsteadiness usually results in large energy losses. This is due to the presence of a strong adverse pressure gradient which causes a rapid growth of the boundary layer along the diffuser wall and its eventual separation from the wall.

The method of prevention of separation in diffusers by boundary layer suction on the divergent walls was first experimentally demonstrated by J. Ackeret[1]. This method was then employed by some investigators[2),3),4)] and showed that a significant improvement on diffuser performance was made.

Another method of improving the diffuser performance is the use of vanes in the diffuser. Cochran and Kline[5)] made an investigation using the short flat vanes in the diffuser, and showed that high pressure recoveries and steady flows were obtained. O. G. Feil[6)] also made an investigation using the vane systems for very wide-angle subsonic diffusers. He tried to arrange the vanes in such a way to translate the source point downstream along the center line to avoid separation and showed that this method is an effective way to improve the performance of wide angle diffusers.

Received May 1, 1974

*Dept. of Mech. Eng., Sci. & Eng. Div., Uni. of the Ryukyus

In previous work[7], tests made with flat vanes in diffusers with divergence angles of 30°, 40° and 60°, developed the basic criteria for effective vane configurations with source point translation. This paper is a continuation of that previous work, and in this study discussions are made on the relation between the pressure recovery and the flow regime. For the 80° diffuser, however, additional discussions are made on the optimum vane configurations.

Nomenclature

A : cross-sectional area of duct
a : spacing between adjacent vanes
b : width of inlet channel
c : distance from plane of diffuser inlet to plane of vane leading edges
L : length of diffuser wall
ℓ : length of vanes
n : number of vanes
p : static pressure
U : velocity outside of boundary layer
u : local x-direction velocity in boundary layer
$\bar{U}$: average velocity in a cross section
x : longitudinal distance along the centerline from the entrance
2θ : total divergence angle
α : total divergence angle between adjacent vanes
C_P : pressure coefficient
C_{PR} : pressurere covery coefficient
η_P : pressure recovery efficient
$\Delta\theta$: anglge for measuring source-point translation
α_w : angle between outer vanes and walls
ρ : density of air
ν : kinematic viscosity
R_{eb} : Reynolds number based on channel width
δ^* : displacement thickness

Subscripts

1 : at an inlet section
2 : at an outlet section where recovery will finish

2. Experimental apparatus and procedure

The experimental apparatus is schematically shown in Figure 1 and details of the diffuser section are shown in Figure 2. The air flow is supplied through an inlet screen

into a test channel by a blower at the downstream exit. The apparatus is formed by the combination of the inlet channel of 60 mm width and 600 mm length, the diffuser with throat aspect ratio of 4:1, and the downstream duct of 240 mm width and 2,800 mm length.

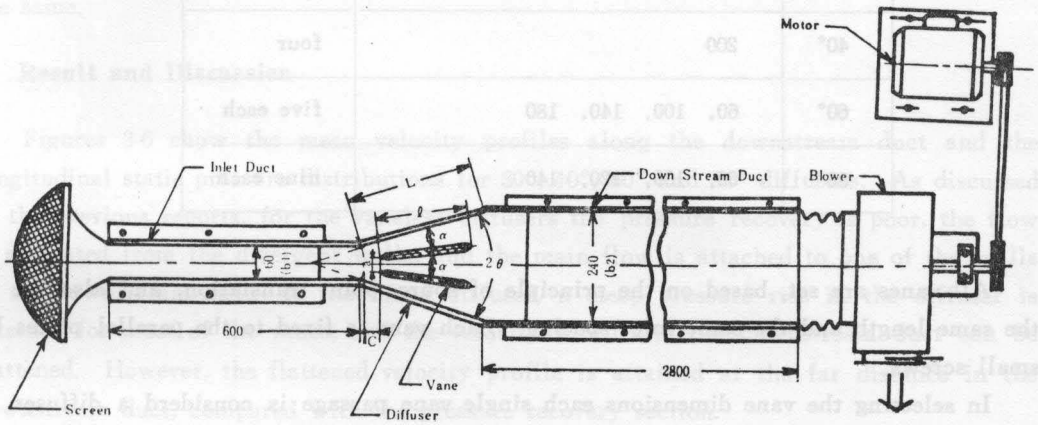

Fig. 1 Schematic view of test apparatus

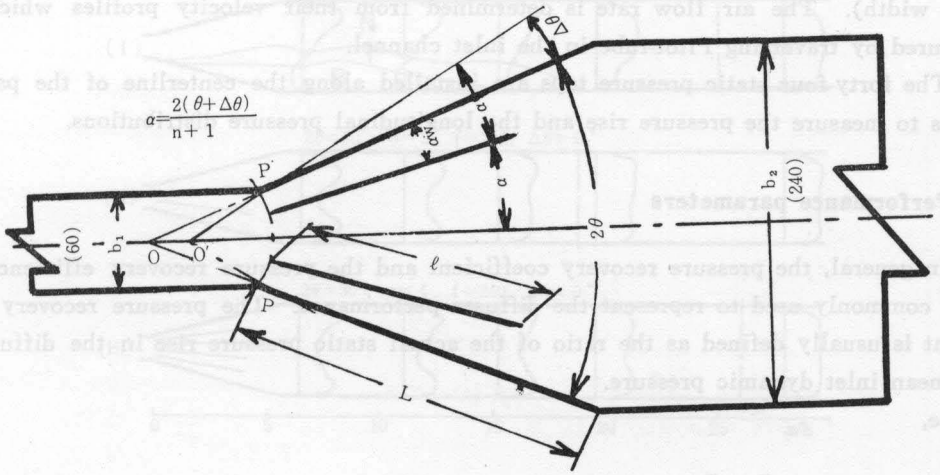

Fig. 2 Diffuser Details

The inlet channel is variable in order to obtain different boundary layer thickness at the diffuser. The top plate of the inlet and the downstream duct are made of 5 mm plexiglass, and the wall tufts are used for flow visualization in all runs.

The vanes are made from sheet metal (2 mm thick) and their dimensions are shown in Table I.

Table 1

2θ	Length of vanes (mm)	Numbers
30°	80, 120, 180, 240, 320, 350	four each
40°	200	four
60°	60, 100, 140, 180	five each
80°	60, 100, 120, 140	nine each

All vanes are set, based on the principle of source-point translation, and also set in the same length and the same inlet spacing. Each vane is fixed to the parallel plates by small screws.

In selecting the vane dimensions each single vane passage is considerd a diffuser in its own right, and one of them is chosen so that the optimum performance is obtained for a vane passage.

Tests were made with 30°, 40°, 60° and 80° diffusers with vane configuration under constant inlet velocity of about 35m/s (Reynolds number of $Reb=1.23\times10^5$ based on the inlet width). The air flow rate is determined from their velocity profiles which are measured by traversing Pitot-tube in the inlet channel.

The forty-four static pressure taps are installed along the centerline of the parallel plates to measure the pressure rise and the longitudinal pressure distributions.

3. Performance parameters

In general, the pressure recovery coefficient and the pressure recovery efficiency are most commonly used to represent the diffuser performance. The pressure recovery coefficient is usually defined as the ratio of the actual static pressure rise in the diffuser to the mean inlet dynamic pressure.

Hence,

$$C_{PR}=\frac{P_2-P_1}{\frac{1}{2}\rho\bar{U}_1^2} \quad \cdots\cdots (1)$$

The pressure recovery efficiency is defined as the ratio of the actual pressure recovery and the ideal pressure recovery coefficient, and is given by

$$\eta_P=\frac{C_{PR}}{C_{PRi}}=\frac{P_2-P_1}{\frac{1}{2}\rho\bar{U}_1^2\left[1-\left(\frac{A_1}{A_2}\right)^2\right]} \quad \cdots\cdots (2)$$

where Cpri is the ideal pressure recovery coefficient.

It will be seen from equation (2) that the Cpr is merely dependent upon the pressure recovery efficieny under diffusers which have equal area ratios. Therefore, in this paper the pressure recovery coefficient is used in reducing the data, since the area ratios are the same.

4. Result and Discussion

Figures 3-6 show the mean velocity profiles along the downstream duct and the longitudinal static pressure distributions for 30°, 40°, 60° and 80° diffusers. As discussed in the previous reports, for the vaneless diffusers the pressure recovery is poor, the flow is separated from the divergent walls, and the main flow is attached to one of the walls in the downstream duct. In the vaned diffuser, a steep pressure rise in the diffuser is attained for most of the vanes, and the velocity profiles in the downstream duct can be flattened. However, the flattened velocity profile is attained at the far distance in the downstream duct, compared with the pressure recovery section.

Figure 3 shows the effect of vanes on the velocity profiles and the longitudinal

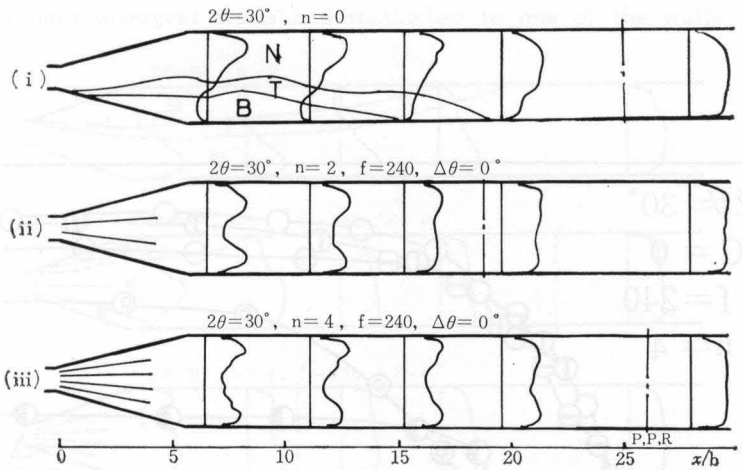

N : No stall region
T : Transitory stall region
B : Back flow region

Fig. 3 Velocity profiles and pressure destributions for 30° diffuser

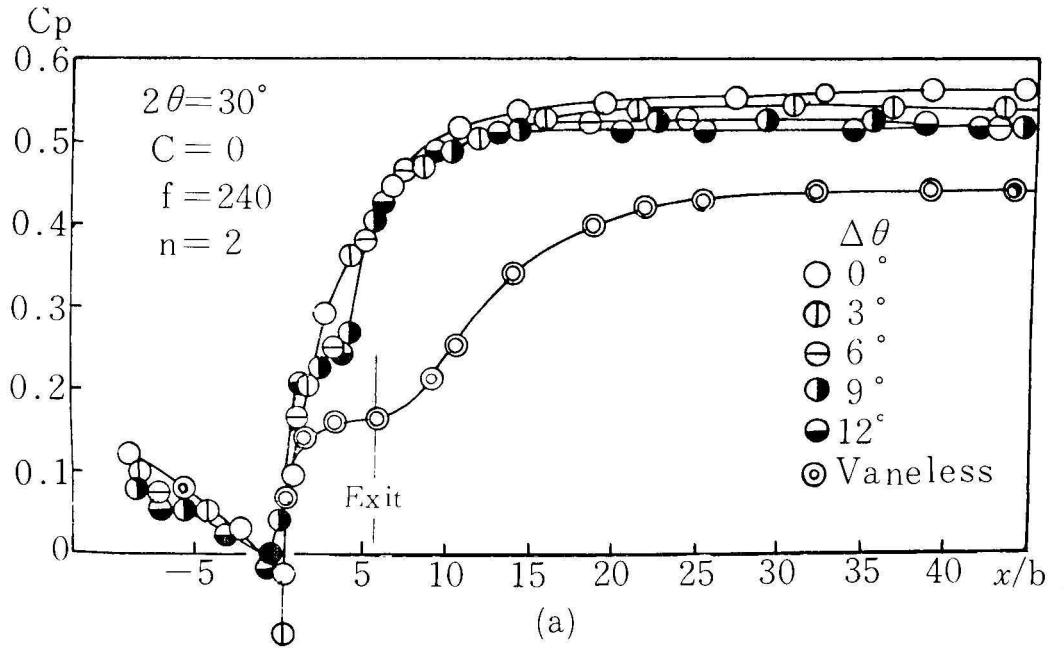
Cp
0.6
0.5
0.4
0.3
0.2
0.1
0
2θ=30°
C=0
f=240
n=2
Δθ
0°
3°
6°
9°
12°
Vaneless
Exit
−5
5
10
15
20
25
30
35
40
x/b

(a)

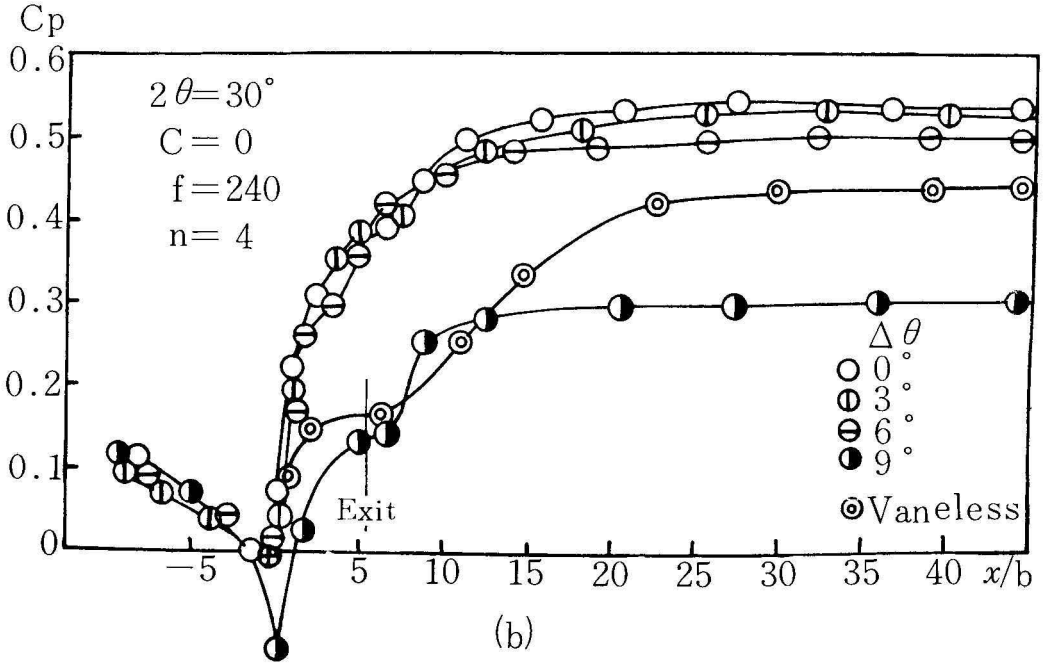
Cp
0.6
0.5
0.4
0.3
0.2
0.1
0
2θ=30°
C=0
f=240
n=4
Δθ
0°
3°
6°
9°
Vaneless
Exit
−5
5
10
15
20
25
30
35
40
x/b

(b)

pressure distributions for the 30° diffuser. As shown in the figure, for the vaneless diffuser the flow is separated from one of the divergent walls and is reattached to the wall in the downstream duct. The main flow is, therefore, attached to the other wall in the downstream duct, and the flow is asymmetrical. However, if vanes are inserted the drift of flow disappears and the flow becomes symmetrical, reducing the back flow regions, for both diffusers with two vanes and four vanes. For the vaned diffusers, the velocity profiles are improved further down into the downstream duct, and the flattened velocity profile is attained at the far distance in the downstream duct. The pressure recovery is also considerably improved everywhere in the diffuser, and the pressure recovery is attained just near the outlet of the diffuser. It should be noted that the pressure recovery in the vaneless diffuser is finished at the near section where the main flow is reattached to the wall. As discussed in the previous reports, the optimum vane configuration in the 30° diffuser on the pressurere covery, is attained for n=2 with ℓ=240. However, there are no evident differences on the velocity profiles between the diffuser with four vanes and the optimum vane configuration, as seen in the figure.

Figure 4 shows the effect of vanes on the velocity profiles and the longitudinal pressure distributions for the 40° diffuser. In the vaneless diffuser, the flow regime is similar to that of the 30° diffuser, and the main flow is attached to one of the walls with larger extent of back flow region. However, if one vane is inserted, the flow is separated from both divergent walls and reattached to one of the walls just near the

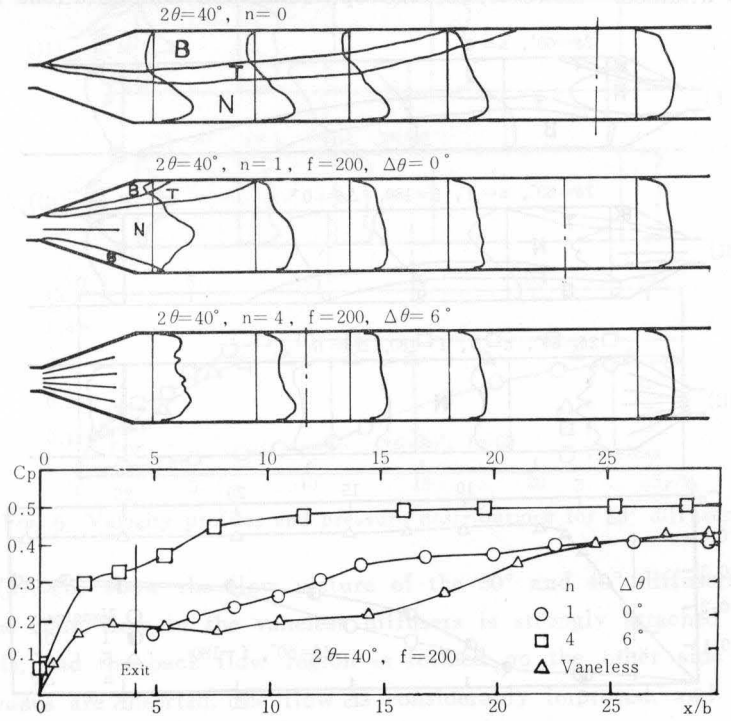

Fig. 4 Velocity profiles and pressure distributions for 40° diffuser

outlet of the diffuser in the downstream duct. For the optimum vane configurations on the pressure recovery, the back flow region disappears and the flow becomes symmetrical, reducing the back flow region. The velocity profiles are also improved in the downstream duct for both vaned diffusers, and are completely flattened near x/b=28.

With regard to the pressure distributions, the diffuser with one vane is still in poor recovery, and the recovery is attained at the far distance in the downstream duct. Here, it is noted that the pressure recovery section will occur near where the flow is reattached. However, in the optimum vane configurations, the pressure recovery is greatly improved, and the recovery is finished near the outlet section of the diffuser.

Figure 5 shows the effect of vanes on the velocity profiles and the longitudinal pressure distributions for the 60° diffuser. In the vaneless diffuser, the flow is separated from both divergent walls, just near the throat, forming a jet flow, and is reattached to one of the walls at a far distance in the downstream duct. For the diffuser with one vane, the back flow region is reduced slightly but still exists on both sides of the walls. However, in the optimum vane configurations the back flow is completely eliminated, and the velocity profiles are flattened as the flow goes down into the downstream duct and is completed at the section x/b=25.

In the vaneless diffuser, the pressure recovery is quite poor, and no pressure rise is observed in the diffuser. The pressure is, however, gradually increased in the downstream duct. For the diffuser with one vane, the pressurere recovery is also quite poor, and no improvement is attained. However, for the optimum vane configurations a remarkable

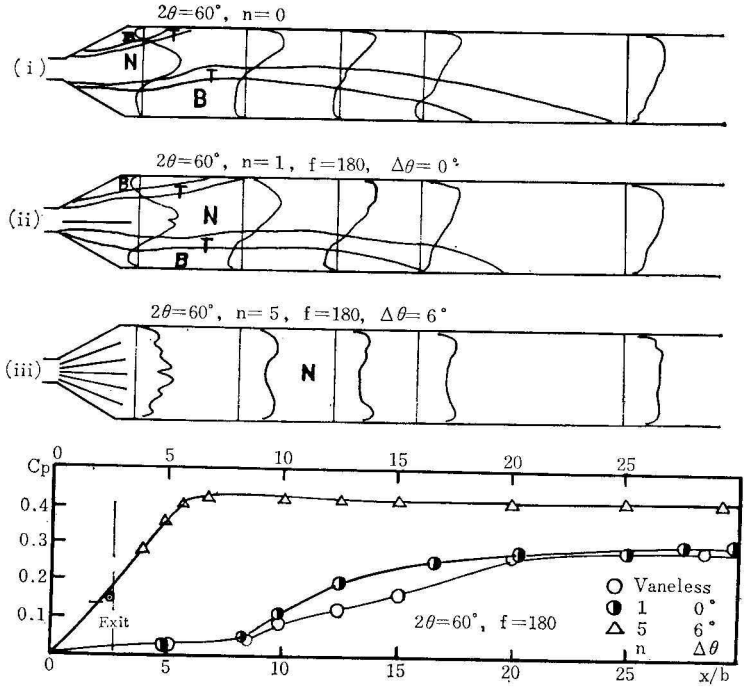

Fig. 5 Velocity profiles and pressure destributions for 60° diffuser

pressure recovery is attained just behind the exit of the diffuser, and no more recovery is observed in the downstream duct.

Figure 6 shows the effect of the vanes on the velocity profiles and the longitudinal pressure distributions for the 80° diffuser. The flow regime is similar to that of the 60° diffuser. However, the back flow region is largely developed in the downstream duct, and the flow reattachment is reached in the section x/b=25. For the vaned diffuser with six vanes and eight vanes, the back flow regions are reduced, but the separation bubbles are still present in both corners at the outlet section of the diffuser. The flattened velocity is also attained in the downstream duct for both vaned diffusers.

The pressure recovery is also similar to the 60° diffuser, and in the vaneless diffuser, the pressure recovery is quite poor. For the vaned diffuser, however, a remarkable pressure recovery is attained behind the exit of the diffuser.

In order to investigate the flow and its separation behavior, sparks of pulverized charcoal are introduced into the flow. Although it can not be said that the flow picture shows exactly the details of the flow because of the inertia of the sparks, it does represent the effect of vanes on flow regimes qualitatively.

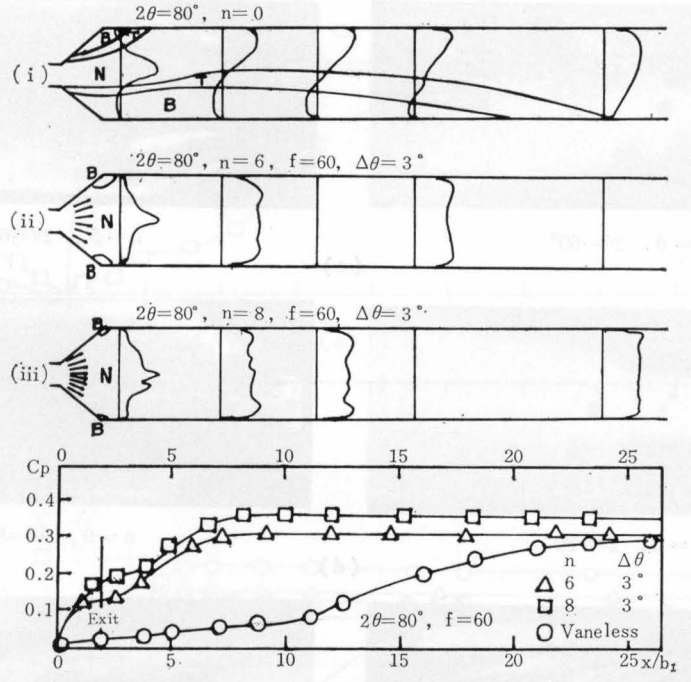

Fig. 6 Velocity profiles and pressure destributions for 80° diffuser

Figure 7 (a), (b) show the flow picture of the 30° and 40° diffusers. As seen in the picture, the main flow in the vaneless diffusers is strongly attached to one of the diverging walls, and the back flow region is formed on the other side of the walls. However, if vanes are inserted, the flow is considerably improved, and the flows are uniform in the downstream duct.

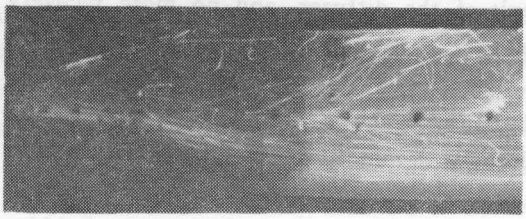

n = 0, 2θ=30°

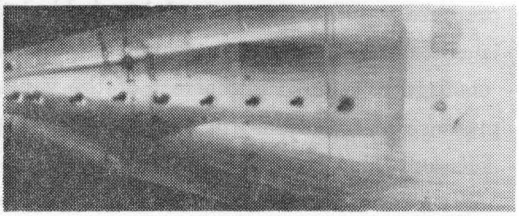

n = 2, 2θ=30°

(a)

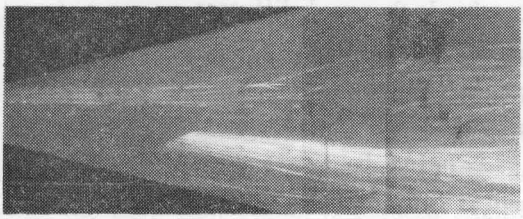

n = 1, 2θ=30°

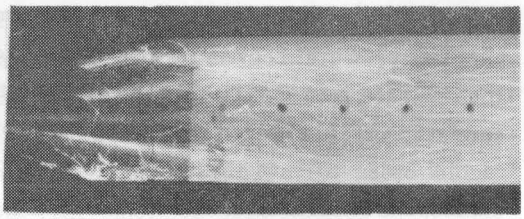

n = 4, 2θ=40°

(b)

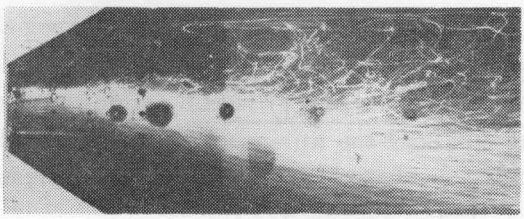

n = 0, 2θ=60°

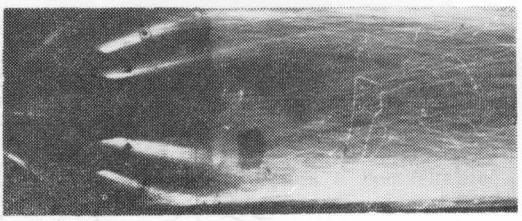

n = 5, 2θ=60°

(c)

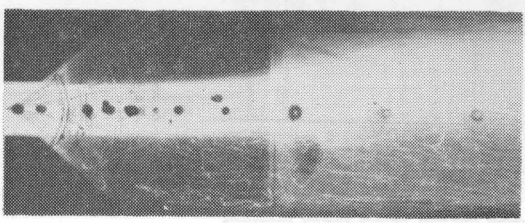

n = 0, 2θ=80°

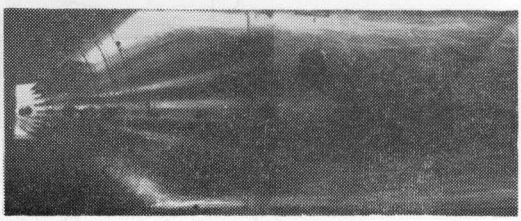

n = 9, 2θ=80°

(d)

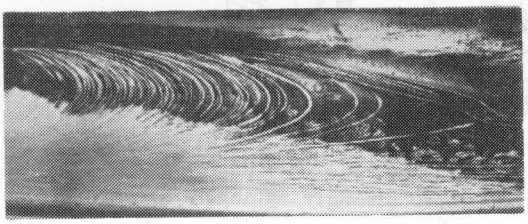

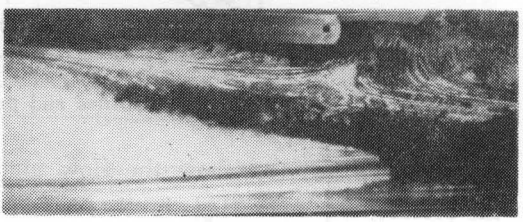

(e)

Fig. 7 The flow picture in the diffuser

Figure 7 (c), (d) show the picture of the 60° and 80° diffusers. In the vaneless diffuser, the approaching flow separates from both diverging walls very near the throat, forming a jet flow, and attaches to one of the walls in the downstream duct. For the vaned diffuser, however, the flow is considerably improved, and the flows are seen to be uniform in the downstream duct.

Figure 7 (e) shows the streak line near in the reattachment section for 30° vaneless diffuser, by using the oil-film method. As seen in the picture, this kind of flow visualization is very effective to determine the reattachment point, and to clarify the mechanism of the eddies in the back Flow region. The flow reattachment point is also checked by tufts and they are consistent with the result in the velocity profiles.

Figure 8 shows the additional tests on the pressure distributions for the 80° diffuser. The same discussions are made in the previous reports for 30°, 40°, and 60° diffusers.

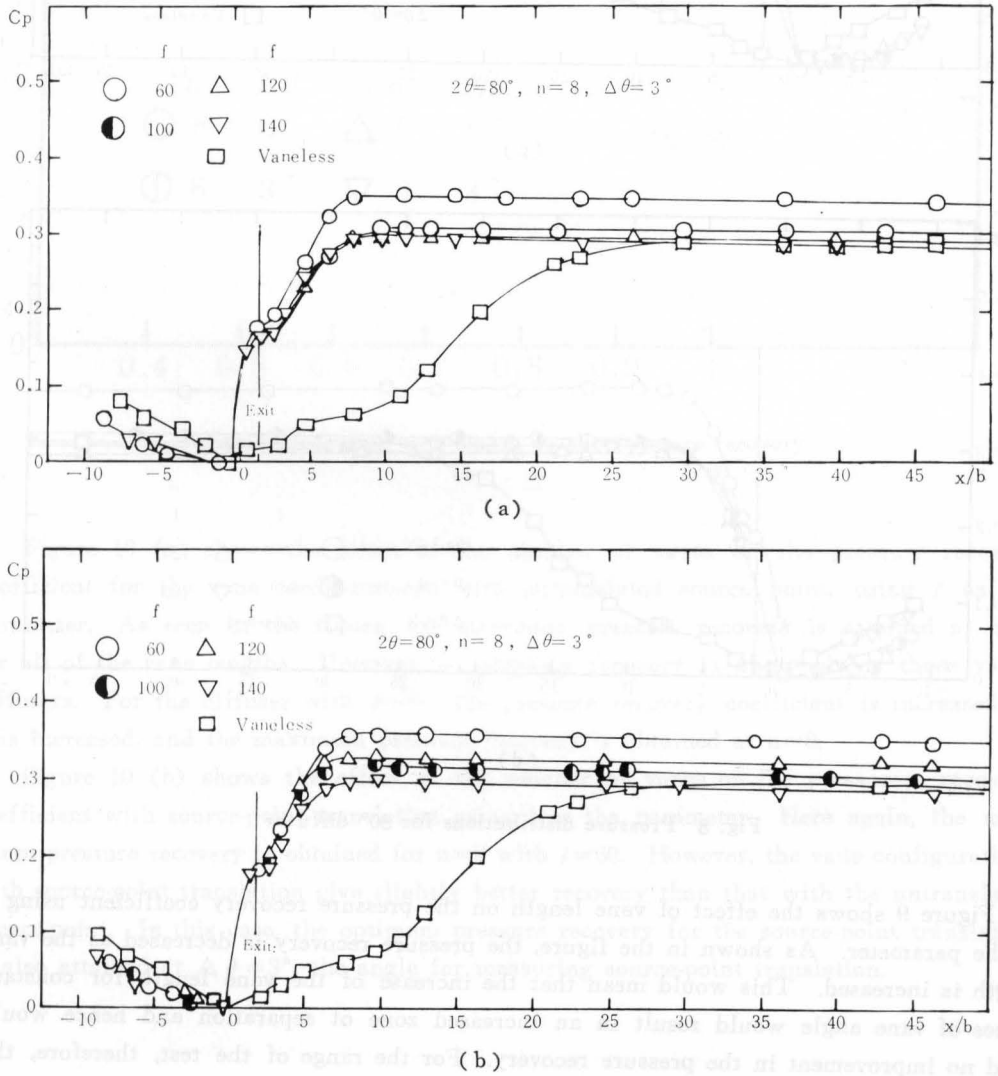

Fig. 8 Pressure distributions for 80° diffuser

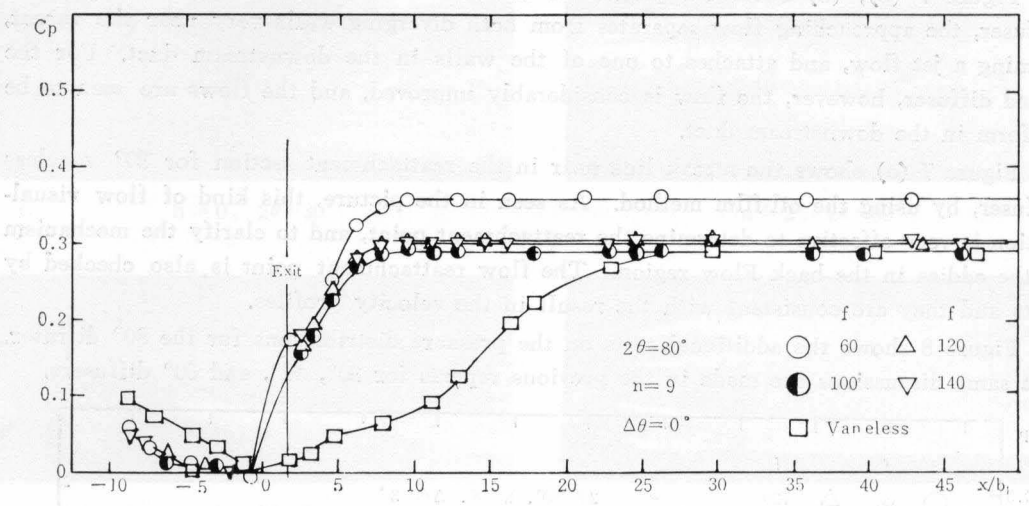

(c)

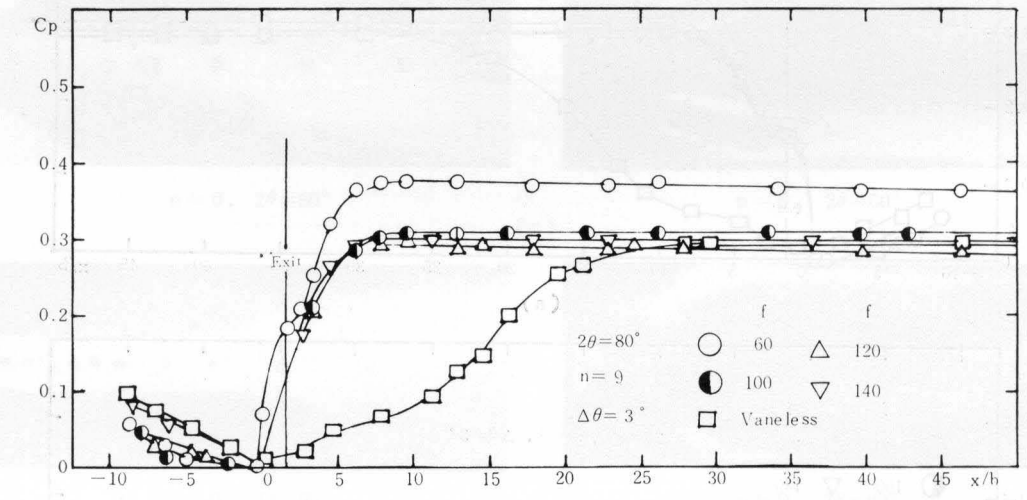

(d)

Fig. 8 Pressure distributions for 80° diffuser

Figure 9 shows the effect of vane length on the pressure recovery coefficient using n as the parameter. As shown in the figure, the pressure recovery is decreased as the vane length is increased. This would mean that the increase of the vane length for constant values of vane angle would result in an increased zone of separation and hence would yield no improvement in the pressure recovery. For the range of the test, therefore, the optimum length of the vane would be $\ell=60$.

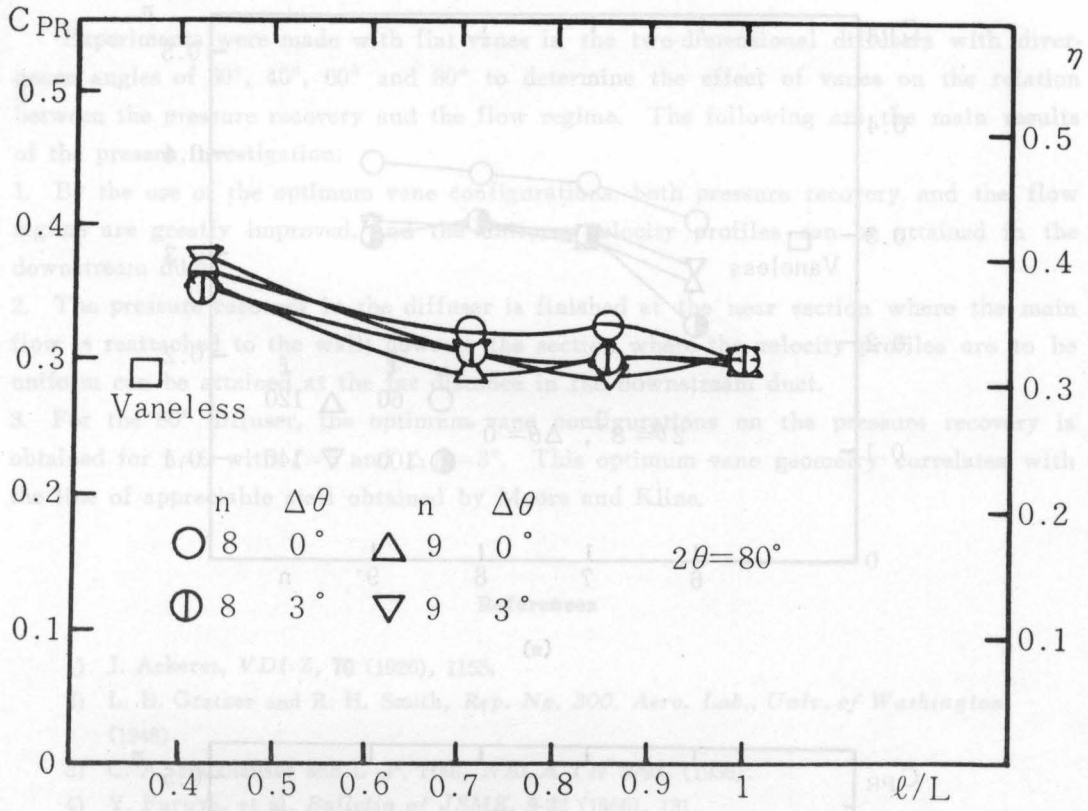

Fig. 9 Effect of vane length on the Pressure recovery

Figure 10 (a) shows the effect of the number of vanes on the pressure recovery coefficient for the vane configurations with untranslated source point, using ℓ as the parameter. As seen in the figure, the maximum pressure recovery is attained at n=8 for all of the vane lengths. However, no pressure recovery is observed for those vaned diffusers. For the diffuser with ℓ=60, the pressure recovery coefficient is increased as n is increased, and the maximum pressure recovery is obtained at n=9.

Figure 10 (b) shows the effect of the number of vanes on the pressurere recovery coefficient with source-point translation using ℓ as the parameter. Here again, the maximum pressure recovery is obtained for n=9 with ℓ=60. However, the vane configurations with source-point translation give slightly better recovery than that with the untranslated source-point. In this case, the optimum pressure recovery for the source-point translation is also attained at $\Delta\theta$=3°, the angle for measuring source-point translation.

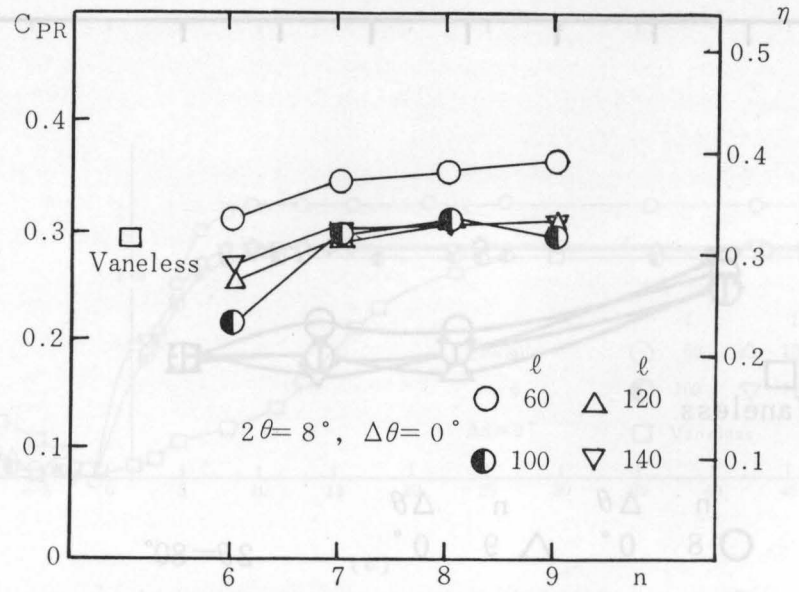

(a)

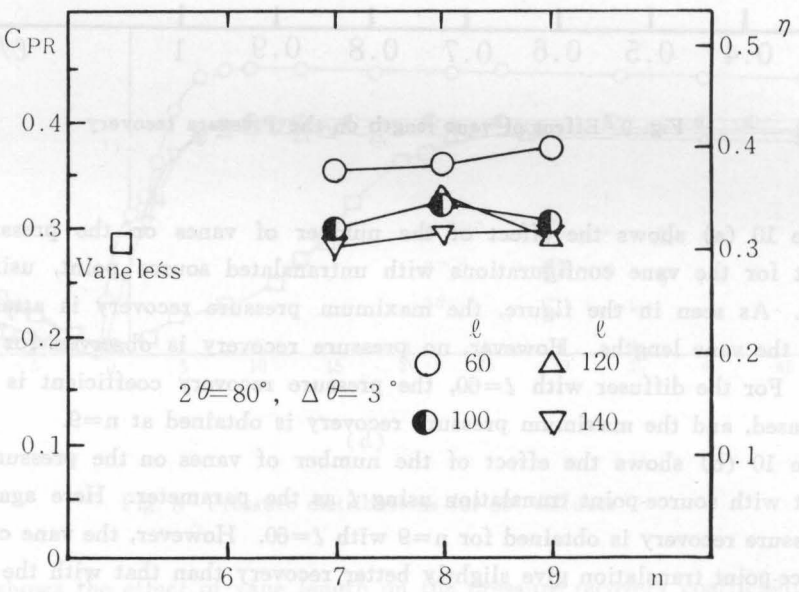

(b)

Fig. 10 Effect of number of vanes on the Pressure recovery

5. Conclusions

Experiments were made with flat vanes in the two-dimensional diffusers with divergence angles of 30°, 40°, 60° and 80° to determine the effect of vanes on the relation between the pressure recovery and the flow regime. The following are the main results of the present investigation:

1. By the use of the optimum vane configurations, both pressure recovery and the flow regime are greatly improved, and the uniform velocity profiles can be attained in the downstream duct.
2. The pressure recovery in the diffuser is finished at the near section where the main flow is reattached to the wall; however the section where the velocity profiles are to be uniform can be attained at the far distance in the downstream duct.
3. For the 80° diffuser, the optimum vane configurations on the pressure recovery is obtained for n=9 with $\ell=6$ and $\triangle\theta=3°$. This optimum vane geometry correlates with the line of appreciable stall obtained by Moore and Kline.

References

1) J. Ackeret, *VDI-Z*, **70** (1926), 1153,
2) L. B. Gratzer and R. H. Smith, *Rep. No. 300, Aero. Lab., Univ. of Washington*, (1948).
3) C. A. Halzhauser and L .P. Hall, *NACA TN* 3793, (1936).
4) Y. Furuya, et al, *Bulletin of JSME*, **9**-33 (1666), 131.
5) D. L. Cochran and S. J. Kline, *NACA TN* 4309, (1958).
6) O. G. Feil, *Trans. of ASME, Sers. D.* **86**-4 (1964), 759.
7) E. Yamazato, and K. Irabu. *Bulletin of Science & Eng. Div., Eng.* No. 6, Univ. of the Ryukyus (1973), 39.